Frustration effects in the disordered system $CsMnFeF_6$, studied by neutron scattering, ac susceptibility, and magnetization measurements

L. Bevaart
Studiecentrum voor Kernenergie, Boeretang 200, B-2400 Mol, Belgium
and Universitaire Instelling Antwerpen, B-2610 Wilrijk, Belgium

P. M. H. L. Tegelaar and A. J. van Duyneveldt
Kamerlingh Onnes Laboratorium der Rijksuniversiteit Leiden, 2311-SB Leiden, The Netherlands

M. Steiner
Hahn-Meitner Institut, Glienickerstrasse 100, D-1000 Berlin 39, Germany
(Received 25 May 1982)

In $CsMnFeF_6$, which has a cubic structure ($a=10.5$ Å), space group $Fd3m$, the magnetic ions Mn^{2+} and Fe^{3+} form regular tetrahedra. The system should exhibit frustration effects, since the nearest-neighbor interactions are antiferromagnetic in character. We performed neutron scattering, ac susceptibility, and magnetization measurements both on a powder and a single crystal, for temperatures $1.2 \lesssim T \lesssim 300$ K and applied magnetic fields $0 \lesssim H \lesssim 50$ kOe. It was found that already at $T=300$ K there are well-developed clusters of antiferromagnetically coupled spins. These clusters have a weak resulting moment. Lowering the temperature to $T \simeq 80$ K leads to an increase of the effective moment due to the reduction of the thermal motions, whereas this moment remains constant for $T \lesssim 80$ K. At $T=26.3$ K the cluster moments freeze in—a process which is accompanied by a ferromagnetic ordering of the resulting moments of the clusters. It is suggested that an applied magnetic field breaks the large domains, containing many clusters, into microdomains containing only a few clusters, or even one.

I. INTRODUCTION

After the discovery of the so-called spin-glass phase in metallic alloys[1] a tremendous amount of work in the field of spin-glasses, superparamagnetism, and disordered systems has been done, both by experimentalists and theorists.[2] Especially the systems *Cu*Mn, *Au*Fe, and *Pd*Mn appear to be good examples to study spin-glass phenomena. A large part of the experimental work done by now can be found in Refs. 2–4, and references therein, while most of the theoretical studies are covered by Ref. 5 and its references, and Ref. 6. The competition due to the long-range Ruderman-Kittel-Kasuya-Yosida (RKKY) interaction causes a frustration with respect to the ordering pattern of the randomly distributed moments of the magnetic ions within the metal lattice. At sufficiently low temperatures the moments of the system do freeze in, resulting in the so-called spin-glass state. Notwithstanding numerous trials, a unique theoretical description of the spin-glass state is not available yet.

A few years ago, examples of crystalline, insulating spin-glasses were found and studied.[7–9] The susceptibilities and specific heats of the samples $FeMgBO_4$, $FeMg_2BO_5$,[7] Fe_2TiO_3,[8] and (Eu,Sr)S (Ref. 9) show remarkable resemblance to those of the metallic spin-glasses. Also it is found that some insulating amorphous compounds behave spin-glass-like [e.g., $MnO{\cdot}Al_2{\cdot}SiO_2$,[10] $PbMnFeF_7$, Pb_2MnFeF_9,[11] and $Pb_2FeMn_{1-x}Zn_xF_9$ (Ref. 12)]. In the insulating compounds the frustration results from competing random *short*-range exchange interactions, in contrast to the *long*-range RKKY interaction effective in metallic compounds.

In this paper we present a neutron scattering, ac susceptibility, and magnetization study on the insulator $CsMnFeF_6$. According to Babel[13] this compound has the space group $Fd3m$, and the magnetic ions Mn^{2+} and Fe^{3+} are randomly distributed on a network of corner-sharing tetrahedra. Since Mn^{2+} and Fe^{3+} both have the spin value $S=\frac{5}{2}$, and since the nearest-neighbor exchange interactions between Mn^{2+}-Mn^{2+}, Mn^{2+}-Fe^{3+}, and Fe^{3+}-Fe^{3+} are all three strongly antiferromagnetic,[14] this system must exhibit so-called frustration effects. Because the ionic radii of Mn^{2+} and Fe^{3+} are substantially different ($R=0.80$ and 0.64 Å, respectively), there

may be a considerable variation in the strengths of the (random) possible superexchange interactions. Moreover, there is a difference in covalency between $Mn^{2+}-F^-$ and $Fe^{3+}-F^-$ bonds, which will also contribute to the random variation in the exchange constants. It is generally assumed that the two properties, *frustration* and *randomness,* are sufficient to bring about spin-glass behavior. Therefore, we anticipated $CsMnFeF_6$ to be an example of an insulating spin-glass, which could also be concluded from the early neutron scattering results obtained by Kurtz,[15] who observed a large amount of diffuse intensity, besides an apparent cusp in the static susceptibility. The new aspects in our studies are the following: (i) experiments on single crystals, (ii) individual measurements performed with better statistics, which enabled us to observe in neutron scattering diagrams very weak peaks that correspond to magnetic long-range order (LRO), (iii) a neutron scattering study of the applied magnetic field (H) dependence of various phenomena, (iv) extra attention paid to the crystallographic features of the substance, (v) ac susceptibility experiments at various temperatures and field values, and (vi) magnetization measurements up to $H=400$ kOe.

The scope of this paper is as follows. In Sec. II some experimental details will be given. Section III is devoted to the presentation of the experimental results, which will be discussed in Sec. IV.

II. EXPERIMENTAL DETAILS

The experiments have been carried out on both powder[16] and single-crystal samples. In Fig. 1 we show the crystallographic structure of $CsMnFeF_6$.[13,14] The structure is face-centered cubic ($a=10.5$ Å at $T=300$ K), space group[17] $Fd3m$, containing a network of corner-sharing $(Mn,Fe)_2F_6$ octahedra, as is shown in more detail in Fig. 1(b). As we will discuss in the next section, the octahedra can be described best by taking into account an anisotropic temperature factor for the F^- ions. The Mn^{2+} and Fe^{3+} ions are randomly distributed and form regular corner-sharing tetrahedra in such a way that every ion is a crossing point of three chains of magnetic ions.

In order to study the magnetic short-range order (SRO) and LRO as a function of T and H, neutron scattering experiments have been performed on the multicounter spectrometer at the BER II reactor of the Hahn-Meitner-Institut in Berlin.[18] We used a monochromated incoming neutron beam with a wavelength $\lambda=2.39$ Å. The multicounter covers a

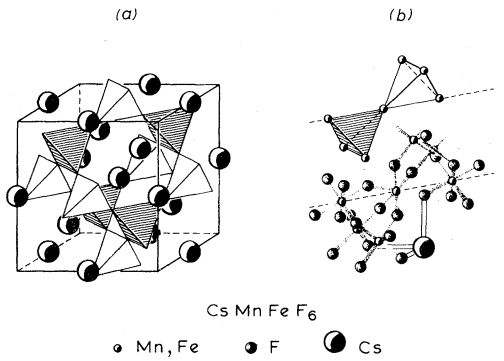

FIG. 1. Crystal structure of $CsMnFeF_6$. In (a) it is shown how the corner-sharing tetrahedra of the magnetic ions are placed in the unit cell, while in (b) the F network is given with respect to the other ions.

scattering angle (2θ) range of 80°, which is divided into 400 channels. We have placed the counter in such a way that it was possible to measure in the interval $5°<2\theta<85°$. However, only the information gained at $5°<2\theta<45°$ was relevant, because of the occurrence of peaks due to the aluminium of the cryostat.

For the measurements we used a standard He-flow cryostat in combination with a superconducting coil, which enabled us to set the temperature in the interval 4.2 K $<T<$ 70 K and at $T=300$ K, in magnetic fields up to $H=50$ kOe. The temperature stability varied from 0.1 K at short terms to 2–3 K at long terms (8 h). A disadvantage of this cryostat is the considerable amount of liquid He in the neutron beam, causing a high background. Consequently, good statistics could only be obtained by extending the measurements over a period of 5–8 h. However, it was not all as wasteful as it appeared, because through the longest runs we were able to observe for $T\lesssim 28$ K small magnetic Bragg peaks. This phenomenon can be related to the onset of magnetic LRO and will be further described in the next section.

For temperatures 70 K $<T<$ 300 K we used a closed-cycle cryostat. The problem of liquid He in the neutron beam did not occur in this configuration, but it was not possible to apply an external magnetic field in this set up. To obtain more detailed information about the crystallographic structure, several spectra have been recorded at various temperatures on the HB-5 two-axes spectrometer at the HFR reactor in Petten, the Netherlands.

Almost all neutron scattering measurements have been carried out on powdered samples. We per-

formed only a few additional selective control measurements on a single crystal and observed no essential differences between the two series of experiments. (We mention that the mosaic spread of the investigated samples is in the order of 1°.)

The T and H dependence of the ac susceptibility, $\chi(T)$ and $\chi(H)$, respectively, have been determined at the Kamerlingh Onnes Laboratory of the University of Leiden. These measurements were done by means of inductance techniques giving a simultaneous recording of the in-phase component of the susceptibility χ' and the out-of-phase component χ''.[19] Mostly, we used a single crystal, which was spark cut into an almost perfect sphere with a diameter of 3.4 mm. The results of $\chi(H)$ did not show a dependence on the direction of H with respect to the crystal axes. This explains why no significant differences arose between the outcomes for the single crystal on the one hand and the powder on the other hand. For 70 K $< T <$ 300 K, χ was determined with a Faraday balance.

The magnetization curves for low H values (up to $H = 4$ kOe) have been obtained in the susceptibility set up, by means of integration of the flux variation upon moving the sample[20] and for large H values (up to $H = 400$ kOe) with a pulsed setup, incorporating a pick-up coil for the flux variation upon varying H.[21]

III. EXPERIMENTAL RESULTS

A. Neutron scattering

1. *Magnetic (dis-)order*

We have measured the powdered sample in zero field for 5 K $< T <$ 300 K. In Fig. 2 a diagram corrected for background at $T = 30$ K is presented. The first striking feature which comes forward is the large amount of diffuse intensity around the (111) peak, in the interval $5° < 2\theta < 45°$, indicating that a large part of the system is not ordered over long ranges but orders within short distances. From the values of the scattering angles it follows that this phenomenon involves either magnetic or nuclear disorder of the magnetic ions. The diffuse intensity does not alter for 5 K $\lesssim T \lesssim$ 70 K. Around 80 K a decrease sets in, which continues up to room temperature, where still a substantial part (about 40%) is present. The width of the diffuse scattering hardly varies. On one hand, the T dependence of the diffuse intensity suggests that the SRO has, at least partly, a magnetic character. The magnetic interactions involved in the ordering process may be so strong that even at room temperature magnetic SRO remains. On the other hand, it might as well be that nuclear disorder (clustering or anticlustering) is responsible for the observed diffuse scattering.

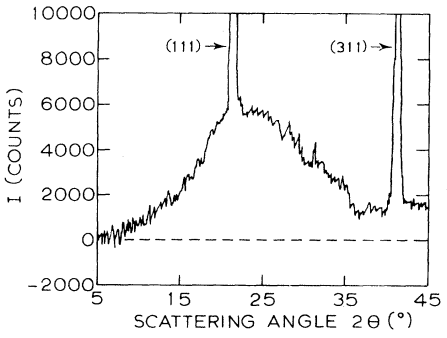

FIG. 2. Neutron scattering scan for $T = 30$ K, corrected for background.

The second feature of Fig. 2 is that the intensity goes to zero when 2θ becomes small. This means that the dominant magnetic interactions involved in the SRO are certainly not ferromagnetic.[22] This was to be expected since the nearest-neighbor exchange interactions between the various magnetic ions are antiferromagnetic. Furthermore, one may conclude that the possible nuclear part of the diffuse scattering does not originate from clustering of identical ions, because in that case we should have observed diffuse intensity at small angles.[22] Consequently, the nuclear contribution to the intensity, if there is any, is a result of anticlustering[22]; i.e., every Mn^{2+} ion is then surrounded by Fe^{3+} ions, and reversely. However, anticlustering is not possible within this crystal structure, and therefore it is not likewise possible that the diffuse intensity has a nuclear origin.

Another interesting outcome is the small difference in the intensity of the (111) peak [Fig. 3(a)], which appears in the spectra for $T \lesssim 25$ K, after comparing these with the one recorded at $T \simeq 70$ K. We note that the (111) nuclear peak is very strong and the difference is due to magnetic ordering in the sample. Since the half-width at half maximum (HWHM) is almost entirely determined by the experimental resolution, the small resulting Bragg peak originates from magnetic LRO. We have not found significant differences between the diagrams in the region 25 K $\lesssim T \lesssim$ 70 K. Because of the relatively large statistical error and temperature insta-

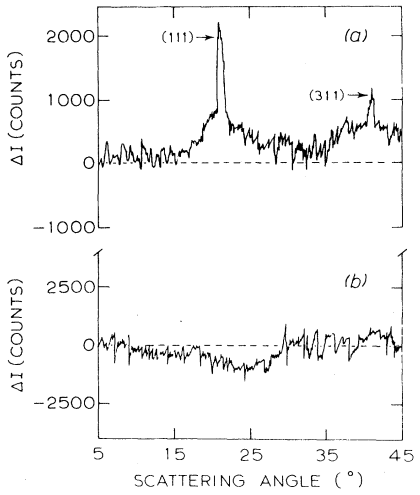

FIG. 3. (a) Difference between a scan at $T=10$ K and one at $T=70$ K, in zero field. (b) Difference between a scan at $T=10$ K and one at $T=70$ K, in $H=20$ kOe.

bility it is not possible to obtain information about the nature of the phase transition near $T\sim 25$ K.

In the study the H dependence of the observed SRO and LRO, we also have performed measurements at $H=2$, 20, and 40 kOe, for 5 K $< T <$ 70 K and at $T=300$ K. No mutual differences were found between the spectra at different H values, so in the following we will discuss the neutron measurements in terms of zero-field and in-field measurements. Furthermore, the applied magnetic field did not affect the diffuse intensity within the experimental accuracy. One can understand this effect by taking into account that the dominant antiferromagnetic exchange interaction is much stronger (as we shall see later) than the applied fields.

The most interesting finding is, however, the disappearance of the small (111) peak after a field has been applied. Once a field has been put on, the peak does not reappear as long as the temperature is not raised above 70 K, even when the field is set to zero. An example of such a scan is given in Fig. 3(b), where scans at $T=10$ and 70 K in a field $H=20$ kOe are compared. One sees that the peak which was present at $H=0$ has disappeared at $H=20$ kOe. After warming up the sample to $T=300$ K, and subsequently cooling it in zero field, we observe again this small magnetic Bragg peak for $T\lesssim 25$ K. The results of the measurements obtained from scans taken after cooling in zero field and in a nonzero field are compiled in Fig. 4, where the intensity of the (111) peak is given for the respective cases. The difference corresponds to the

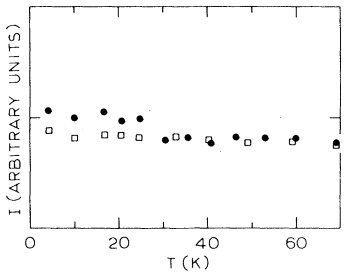

FIG. 4. Intensity of the magnetic (111) peak as a function of temperature, after cooling in zero field (●), and after cooling in $H=20$ kOe (□). The latter corresponds to the intensity of the (111) nuclear peak.

intensity of the magnetic Bragg peak. Since we get our information from two peaks only, and since in the unit cell of this compound there are two magnetic ions, we cannot decide from these data whether the origin of the peak is ferromagnetic or antiferromagnetic LRO.

2. *Nuclear (dis-)order*

In Fig. 5 we show a powder diagram which is obtained at $T=160$ K with the two-axes spectrometer HB5 at the HFR reactor in Petten. With the aid of a profile refinement program[23] the peak data were fitted, taking into account that within the *Fd3m* space group the Cs^+ ions occupy the 8 *b* sites, the magnetic ions the 16 *c* sites, and the F^- ions the 48 *f* sites.[13] Assuming all temperature factors B to be isotropic, we found quite a good agreement between the calculated and the measured diagrams for $2\theta < 100°$. Nevertheless, large differences appear for $2\theta > 100°$, resulting in an R factor of $R\simeq 28$. These discrepancies disappear considerably after introducing an anisotropic temperature factor[24] for the F^- ions in the refinement program[23–25] yielding $R\simeq 10$. In the Appendix we discuss briefly the symmetry relations among the coefficients of the anisotropic temperature factor B of the F^- ions.

In Table I the relevant results of the refinement are summarized for all the measured diagrams. As can be deduced from the Appendix and from Table I, the "thermal motions" of the F^- ions take place mainly along the [111] direction. In other words, one can also state that the F octahedra are randomly elongated or shortened along the [111] direction. Another conspicuous feature in Fig. 5 is the occurrence of two broad maxima around the scattering angles $2\theta\simeq 50°$ and 65°. The shape and size of these maxima of diffuse intensity do not depend on

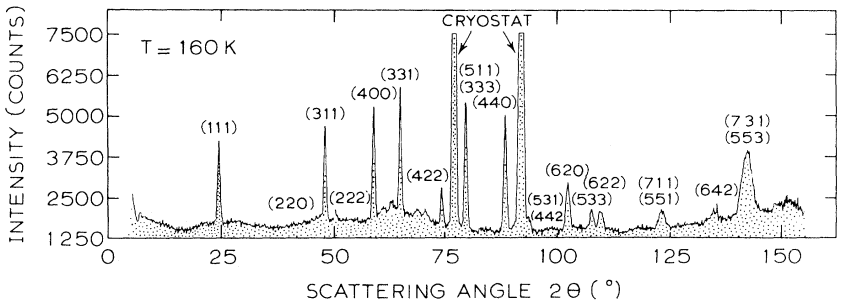

FIG. 5. Neutron scattering diagram, recorded at the HFR reactor in Petten, for $T=160$ K.

T, so the disorder to which these are related has no magnetic character, but is probably due to a miss stacking of particular ions. Because the centra of these maxima correspond roughly with the (Mn,Fe)-F and Cs-F distances, respectively, it is likely that they originate from uncertainties in these distances. Remembering the relatively large temperature factor of F, one could more or less expect the observed diffuse intensities.

B. ac susceptibility and magnetization measurements

The reciprocal ac susceptibility in zero field, $\chi^{-1}(0)$, is depicted in Fig. 6 as a function of T. At $T\simeq 300$ K the increase of $\chi^{-1}(0)$ is still not linear with temperature. However, from extrapolating the high-temperature part, one obtains for the Curie-Weiss temperature the value $\Theta=-285(5)$ K, and for the Curie constant the value $C=9.0(1)$ emu K/mol. The latter value agrees nicely with the theoretical (spin-only) value of $C=8.76$ emu K/mol.

In Fig. 7 we present the T dependence of χ' for different H values, with $\vec{H}$ parallel to the [111] direction. It is noteworthy that $\chi(0)$ as well as $\chi(H)$ does not depend on the strength of the small amplitude of the ac field for $h \lesssim 1.0$ Oe. The curves for $H=0$ and $H=100$ Oe in Fig. 7(a) are very similar to those of ferromagnetic compounds. The susceptibility at $H=0$ diverges at $T_c=26.3$ K. Furthermore, it should be noted that $\chi(T=T_c)$ reaches a value which is only 10% below that of the reciprocal demagnetizing factor of a sphere. For higher H values, however, the shape of the susceptibility versus temperature curve changes dramatically. In Fig. 7(b) one sees that, for $H=556$ and 1560 Oe at T_c, a maximum is built up which decreases and broadens with increasing H. Moreover, the maximum shifts to higher T with higher H. On the other hand, for lower T the χ' rises again. These values in turn also fall off with increasing H. The curves given in Fig. 7 can be understood on the basis of domain-wall movements, as will be discussed in the next section.

In Figs. 8(a) and 8(b) the dependence of χ' and χ'' at $T=4.2$ K on the frequency ν of the ac tickling field is shown. We see that there is a gradual increase of χ'' and decrease of χ' with increasing ν. This behavior suggests that a broad band of relaxation times occurs due to the domain effects, which

TABLE I. Results of the free parameters obtained from the profile refinement of the diagrams recorded in Petten. We note that $y(F)$ and $z(F)$ are both fixed at $\frac{1}{8}$. The temperature factors are given in Å^{-2}.

	$T=4.2$ K	$T=80$ K	$T=160$ K	$T=300$ K
Axes (Å)	10.491	10.504	10.522	10.554
x (F)	0.3193	0.3182	0.3183	0.3182
B (Cs)	2.10	2.31	2.07	3.70
B (Mn + Fe)	2.83	1.65	1.54	1.20
B_{11} (F)	0.0062	0.0060	0.0060	0.0070
B_{22} (F)$=B_{33}$ (F)	0.0221	0.0191	0.0163	0.0134
B_{23} (F)	0.0140	0.0118	0.0111	0.0070
R	11.46	8.16	9.68	9.27

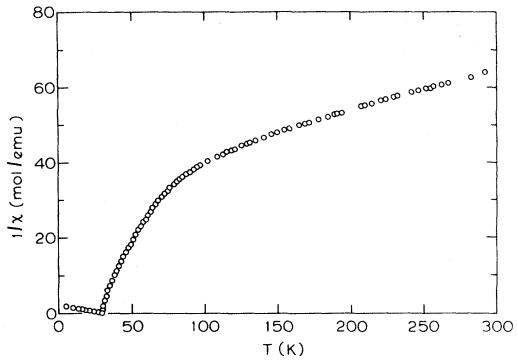

FIG. 6. Inverse zero-field susceptibility as a function of temperature.

is usual for ferromagnetic systems.[26,27]

The magnetization curves as a function of H (<3 kOe) are given in Fig. 9 for various T. A sharp increase of M is seen at weak fields, while for $H>1.5$ kOe all M curves increase linearly with H. Furthermore, at $T=4.2$ K there is a small spontaneous magnetization, whereas no such phenomenon is measured for $T\gtrsim 20$ K. For $T=29.5$ K a linear increase of M as a function of H through ($H=0$, $M=0$) is observed, which indicates that the system is in the paramagnetic phase.

In addition, we mention that for the powder at $T=4.2$ K, magnetization measurements have been performed in pulsed fields up to $H=400$ kOe. Even at the highest H value the sample is not saturated. If one assumes the magnetization to proceed linearly to its saturation value, one is able to estimate the exchange field H_E according to mean-field theory[28] to be ~ 1100 kOe.

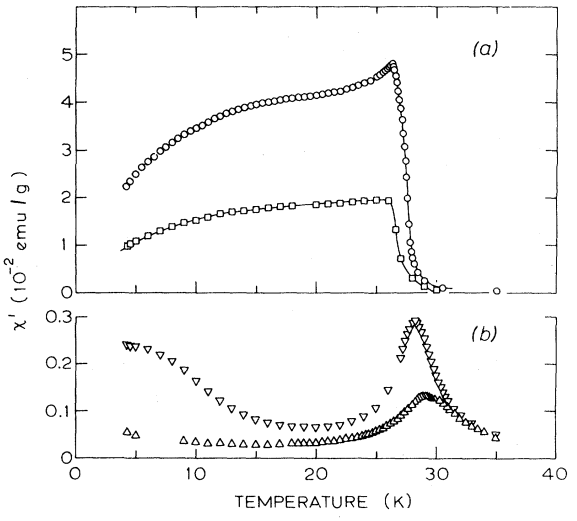

FIG. 7. ac susceptibility at 234 Hz as a function of temperature for different H values: ○ $H=0$; □, $H=100$ Oe; ▽, $H=560$ Oe; △, $H=1560$ Oe.

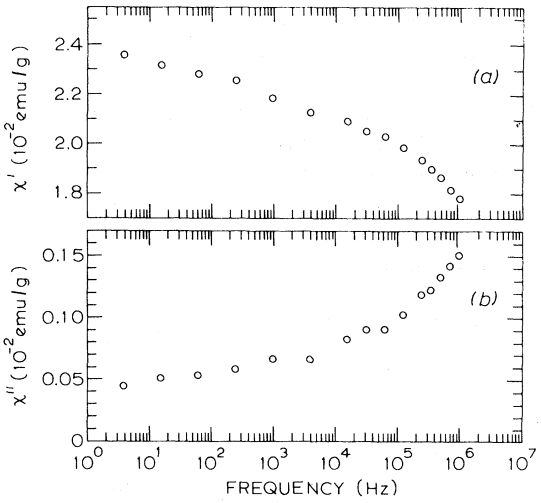

FIG. 8. Dependence on the frequency ν of (a) the dispersion χ' and (b) the absorption χ''.

IV. DISCUSSION

In the cubic material $CsMnFeF_6$, whose space group is $Fd3m$, the magnetic ions Mn^{2+} and Fe^{3+} occupy the 16 c positions. More precisely, they are randomly distributed over corner-sharing regular tetrahedra. From our $\chi(H=0)$ we determined a Curie-Weiss temperature $\Theta=-285$ K, which indi-

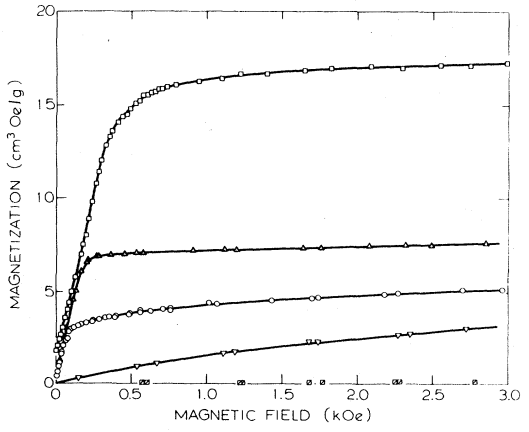

FIG. 9. Magnetization as a function of applied magnetic field, for different temperatures: □, $T=4.2$ K; ▲, $T=20$ K; ○, $T=26.3$ K; ▽, $T=29.5$ K; ⊠, $-T=35$ K.

cates that the nearest-neighbor interaction between the magnetic ions are strongly antiferromagnetic, in agreement with the results found by others.[14,15] Although the interactions favor an antiferromagnetic ordering of the spins, such an ordering is not possible within the crystallographic structure. In the case where the preferred magnetic order cannot be established because of external factors, such as geometric ones, the system will show so-called frustration effects. Consequently, the ground state of the system will be highly degenerate. One of the possible structures is a canted antiferromagnetic one.[29]

The occurrence of magnetic diffuse intensity in the neutron scattering diagrams at $T=300$ K proves that already at room temperature magnetic clusters are present. The clusters involve about 20 spins, which were also found by Kurtz.[15] Since the width of the diffuse intensity decreases only a little for lower T, one might suppose that the size of the clusters hardly increases. However, the maximum increases with T decreasing to 80 K, indicating that the effective magnetic moment of the cluster grows, due to the reduction of the thermal fluctuations of the individual spins. As mentioned before, the manganese and iron spins within a cluster try to approach a complete antiferromagnetic ordering, which may result in a canted structure. This in turn causes every cluster to have a small resulting moment. From the neutron scattering experiments it becomes clear that these "paramagnetic"' clusters freeze in around 25 K. Apparently, this process is accompanied by a ferromagnetic ordering of the small resulting moment of the clusters, as can be evidenced from the character of the χ measurements. The magnitude of the ferromagnetic moment can be estimated by extrapolating the strong field magnetization at $T=4.2$ K to $H=0$. This yields a canted moment of 16 emu Oe/g ($=2.26\mu_B$ per spin) corresponding to a canting angle of $\sim 3°$.

As mentioned before, the small magnetic Bragg peak, obtained for $T<25$ K after cooling in zero field, disappears when a field is applied. The peak does not reappear, when T is cycled between 5 and 70 K, even for $H=0$. However, the peak appears again after cooling from $T=300$ K in zero field. This phenomenon can be explained as follows. Cooling the sample results in a sort of blocking of clusters. Within a domain containing many clusters the spins are aligned antiferromagnetically as good as possible. This quasiantiferromagnetic LRO most likely gives rise to the magnetic Bragg peak. Putting on a field causes the ferromagnetic resulting moments of the clusters to line up along the field direction. This process is accompanied by a rotation of the individual spins in the clusters, and thus will destroy the antiferromagnetic LRO. In other words the domains, consisting of enough clusters to give rise to an antiferromagnetic Bragg peak in the neutron diagrams, split into microdomains consisting of a few clusters, or even one. In neutron scattering this should lead to an increase of the diffuse intensity, but since the integrated intensity in the Bragg peak is very small compared to the diffuse one, the increase is lost in the statistical fluctuations. The susceptibility and magnetization did not show an irreversible effect upon applying a magnetic field. These quantities are not affected by the splitting of domains into microdomains, as is to be expected since with these techniques the bulk properties are determined.

In Sec. III it was already mentioned that the susceptibility and magnetization measurements can be explained in terms of moving domain walls. The curves depicted in Fig. 7(a) show that at zero field the domains are flexible enough to follow the ac field at all temperatures. However, for $H>500$ Oe ($T<T_c$) the domain walls are pinned by the field, yielding a decrease of χ. Because the ferromagnetic moments are more fixed at stronger fields, $\chi_{\max}$ decreases with increasing H. For field values which are high enough, only the antiferromagnetic contribution will be seen. Because of the cubic symmetry of the crystal, we measure a mean value of the antiferromagnetic parallel and perpendicular susceptibility, causing a cusplike form of χ at strong-field values [see, for example, the curves shown in Fig. 7(b)].

From the magnetization measurements at 4.2 K the exchange field H_E was estimated to be 1100 kOe. One may also derive this field from the Curie-Weiss temperature, as in the molecular-field model H_E equals $3k\,|\Theta|/(S+1)g\mu_B$.[28] The Curie-Weiss temperature of -285 K as extrapolated from Fig. 6 then leads to $H_E=1800$ kOe. It should be noted that $\chi^{-1}(0)$ is still not linear with T at $T=300$ K, and that the sample is still not saturated for $H=400$ kOe at $T=4.2$ K, so the respective values of H_E are rough estimates only. On the other hand, it is likely that the mean-field theory is not appropriate for describing a system exhibiting such microscopic disorder. Nevertheless, the present results suggest the antiferromagnetic exchange interaction between neighboring spins to be of the order of -6 K.

From the anisotropic temperature factor, result-

ing from the profile refinement of neutron scattering diagrams, we know that the F octahedra are deformed along the $[11\bar{1}]$ direction. This seems not to be in disagreement with the findings of Babel *et al.*,[16] who concluded that the F octahedra must be compressed along the [111] direction.

Summarizing the above, one can state the following: Even at $T=300$ K, the magnetic interactions are strong enough so that clusters are developed. The nearest-neighbor interaction is antiferromagnetic, and consequently, due to the frustration, the spins within the clusters are canted, which results in a weak moment of each cluster. The individual moments gradually grow with lowering the temperature to $T\simeq 80$ K. For $T\lesssim 80$ K these moments do not change within the experimental accuracy. It is noteworthy that we did not detect a phase transition at $T\simeq 80$ K. At $T=26.3$ K the clusters freeze in and form canted antiferromagnetic domains. Their net moments order ferromagnetically, possibly due to dipolar interactions. An external magnetic field breaks the domains of the canted antiferromagnetic clusters, into microdomains.

In concluding this section, we would like to compare our results with those of Maletta *et al.* for the system $Eu_xSr_{1-x}S$.[9,20] In these compounds, the random competing ferromagnetic and antiferromagnetic interaction causes the freezing in of the so-called spin-glass state. For $x\leq 0.5$ they observe for $T>T_c$ ferromagnetic SRO, whereas for $T<T_c$ the blocked microdomains form the spin-glass phase.[9] For $x>0.54$, they find below T_c long-range ferromagnetism, in combination with ferromagnetic microdomains. The interesting interval is $0.5<x\leq 0.54$, where for $T<T_c$ also the mixed phase of ferromagnetic LRO and SRO is reached. However, for sufficiently low temperatures the LRO disappears and the microdomains freeze in.[30] It should be noted that the resemblance between the χ curves, shown in Ref. 30, which are explained in spin-glass terms, and the χ curves given by us in Fig. 7 is remarkable.

In $CsMnFeF_6$, the difference between the ionic radii of Mn^{2+} (0.80 Å) and Fe^{3+} (0.64 Å) amounts to about 3% of the distance between the magnetic ions. Since the superexchange is very sensitive to the ion radii[31] the various exchange constants may differ a lot. This effect, together with the difference in covalency between the $Mn^{2+}-F^-$ and $Fe^{3+}-F^-$ bonds, yields a random distribution of exchange integrals. In combination with frustration this should lead to a spin-glass phase. However, our results can be reasonably explained in terms of clusters, domains, and microdomains. So one might argue about the nature of a spin-glass phase. Maybe a spin-glass is just a very complicated antiferromagnet with the unit cell as large as the sample. It is clear that a lot of work must be done for a complete understanding of magnetic ordering phenomena, which cannot be described as paramagnetism or as usual long-range order. In this context we are now studying the specific heat. Also the frequency—time-dependent behavior of both χ and M is being examined in more detail, together with the irreversible component of the magnetization and the way in which this component depends on the magnetic history of the sample. A model description for M, M_{irrev}, and χ of metallic spin-glasses along the same lines is in press.[32]

ACKNOWLEDGMENTS

The neutron scattering experiments on the multicounter spectrometer have been performed in the year that one of us (L.B.) worked as a guest scientist at the Hahn-Meitner Institut in Berlin. We are indebted to Professor D. Babel and co-workers, and Dr. B. Wanklyn for preparing the powdered and single-crystal samples, respectively. The Solid State Group of the Netherlands Energy Research Foundation in Petten is acknowledged for their hospitality during the time necessary to analyze the recorded diagrams. Dr. L. J. De Jongh kindly performed the high-field magnetization measurements, while Dr. J. van Nieuwkoop recorded some susceptibility data on a powdered sample, which encouraged us to proceed with the present research. Furthermore, we are obliged to Dr. W. Engelfriet, who carried out the high-temperature susceptibility measurements with the Faraday balance. The discussions with Dr. B. van Laar and Dr. H. A. Groenendijk were very fruitful. One of us (L.B.) thanks the Belgian Interuniversitair Instituut voor Kernwetenschappen for making it possible for him to participate in this study.

APPENDIX: SYMMETRY RELATIONS BETWEEN THE COEFFICIENTS OF THE ANISOTROPIC TEMPERATURE FACTOR OF F

The definition of the temperature factor $\exp(-M_{\vec{h}})$ is given by[24]

$$M_{\vec{h}}=\sum_{i=1}^{3}\sum_{j=1}^{3}B_{ij}h_ih_j, B_{ij}=B_{ji}\ .$$

Here $\vec{h}=\sum_{i=1}^{3}h_i\vec{b}_i$ is the reciprocal-lattice vector for the reflection in question. We note that we have denoted B_{ij} in our paper as the temperature factor.

$CsMnFeF_6$ has space group $Fd3m$, with the F^- ions occupying the 48 f positions. The symmetry elements which leave the 48 f positions invariant are the following:

$$q_1:\ x,y,z,\longrightarrow x,z,y,$$

$$q_2:\ x,y,z\longrightarrow x,\tfrac{1}{4}-y,\tfrac{1}{4}-z\ .$$

From this one obtains for these positions: $(x,\frac{1}{8},\frac{1}{8})$. It is noteworthy that, within this space group, x is a free parameter.

From the quadratic products (cf. Ref. 24) of these symmetry operations one can determine that $B_{22}=B_{33}$ and that $B_{12}=B_{13}=0$. Thus one obtains the determinant

$$\begin{vmatrix} B_{11} & 0 & 0 \\ 0 & B_{22} & B_{23} \\ 0 & B_{23} & B_{22} \end{vmatrix},$$

which gives, as eigenvalues, B_{11}, $B_{22}+B_{23}$, and $B_{22}-B_{23}$. These, in turn, determine the eigenvectors [100], [011], and [01$\bar{1}$], respectively. Combining this with the values for B given in Table I, we conclude that the F octahedra are smeared out along the [11$\bar{1}$] direction.

[1]V. Cannella and J. A. Mydosh, Phys. Rev. B 6, 4220 (1972).

[2]See, for instance, Proceedings of the International Conference on Magnetism, Munich, 1979 [J. Magn. Magn. Mater. 15-18 (1980)]; and Proceedings of Low Temperature Physics Lt-16 [Physica B + C 107 + 108 (1981)].

[3]J. A. Mydosh, J. Magn. Magn. Mater. 7, 237 (1978).

[4]A. P. Murani, J. Appl. Phys. 49, 1604 (1978).

[5]A. Blandin, J. Phys. C 6, 1499 (1978).

[6]Proceedings of the International Conference on Disordered Systems and Localization [J. Magn. Magn. Mater. (in press)].

[7]A. Wiedenmann and P. Burlet, J. Phys. C 6, 720 (1978).

[8]U. Atzmony, E. Gurewitz, M. Melamud, H. Pinto, H. Shaked, G. Gorodetsky, E. Hermon, R. M. Hornreich, S. Shtrikman, and B. Wanklyn, Phys. Rev. Lett. 43, 782 (1979).

[9]H. Maletta and W. Felsch, Phys. Rev. B 20, 1245 (1979).

[10]J. P. Renard, J. Pommier, J. Ferre, and K. Knorr, J. Phys. C 6, 936 (1978).

[11]J. P. Renard, J. P. Miranday, and F. Varret, Solid State Commun. 35, 41 (1980).

[12]C. Dupas, K. le Dang, J. P. Renard, P. Veillet, J. P. Miranday, and C. Jacoboni, J. Phys. (Paris) 42, 1345 (1981).

[13]D. Babel, Z. Anorg. Allg. Chem. 387, 161 (1972).

[14]E. Banks, J. A. Deluca, and O. Berkooz, J. Solid State Chem. 6, 569 (1973).

[15]W. Kurtz, Ph.D. thesis, University of Tübingen, Tübingen, W. Germany, 1977 (unpublished); W. Kurtz and S. Roth, Physica 86-88B, 715 (1977).

[16]D. Babel, G. Pausewang, and W. Viebahn, Z. Naturforsch. 22B, 1219 (1967).

[17]Space group No. 227 in *International Tables for X-ray Crystallography*, edited by N. F. M. Henry and K. Londsdale (Kynoch, Birmingham, England, 1952), Vol. I.

[18]A. Axmann, Hahn-Meitner Institut Report No. HMI-B257 (unpublished).

[19]A. J. de Vries and J. W. M. Livius, Appl. Sci. Res. 17, 31 (1967); H. A. Groenendijk, A. J. van Duyneveldt, and R. D. Willett, Physica 101B, 320 (1980).

[20]This set up was built by I. Wanga, and is described in his graduate thesis (unpublished).

[21]H. A. Jordaan, R. Wolf, and D. de Klerk, Physica 69, 129 (1973).

[22]J. Vrijen, Ph.D. thesis, University of Utrecht, Utrecht, The Netherlands, 1977 (unpublished), and ECN Report No. ECN-31, Petten, The Netherlands.

[23]H. M. Rietveld, J. Appl. Crystallogr. 2, 65 (1969).

[24]A. Levy, Acta Crystallogr. 9, 679 (1956).

[25]A. W. Hewat, Harwell Report No. AERE-R7350 (unpublished).

[26]I. Maartense, Solid State Commun. 9, 2071 (1971).

[27]A. A. Galkin, V. P. Djykonov, I. M. Fita, and G. A. Tsintsadze, Phys. Lett. 68A, 263 (1978).

[28]See, e.g., R. L. Carlin and A. J. van Duyneveldt, *Magnetic Properties of Transition Metal Compounds* (Springer, New York, 1977).

[29]J. Villain, Z. Phys. B 33, 31 (1979).

[30]D. Meschede, F. Steglich, W. Felsch, H. Maletta, and W. Zinn, Phys. Rev. Lett. 44, 102 (1980).

[31]L. J. de Jongh and R. Block, Physica 79B, 568 (1975).

[32]A. J. van Duyneveldt and C. A. M. Mulder, Physica 114B, 82 (1982).